7th Int'l CFB Conference, Niagara Falls, New York, pp. 255-262

Circulating Fluid Bed Operating Regimes

Lawrence J. Shadle*, Esmail R. Monazam++, and Joseph S. Mei*
National Energy Technology Laboratory
***U. S. Department of Energy**
3601 Collins Ferry Rd.
Morgantown, West Virginia 26507-0880
++REM Engineering
3566 Collins Ferry Rd.
Morgantown, West Virginia 26505

Abstract

A Cold Flow Circulating Fluid Bed (CFCFB) having diameter of 0.3 m-ID and 15 m-high riser, was operated under ambient conditions and different fluidization flow regimes. Identification of fluidization flow regimes and their boundaries is critical to CFB operation and performance. Atmospheric circulating fluid bed combustors operate in the fast fluidization flow regime; however, significant improvements to reactor thruput and thus capital costs that are possible with combustors operating in the dense transport regimes. Flow instabilities are observed in riser pressure fluctuations and the solids circulation rates when operating in the intermediate, turbulent and fast fluidization flow regimes. In this work the flow regimes were studied from homogeneous dilute-phase flow regime to dense-phase fluidization flow regime. Coarse cork particles were employed in the experiments to facilitate computational fluid dynamic model validation. Interpretation of results in time domain pressure differentials and solids circulation data were used to identify the flow regimes. The method was to increase the solid flow rates by increasing the aeration air to the nonmechanical valve (a loop seal) while maintaining a given riser gas velocity. The effects of gas velocity and solid circulation rate were evaluated. Operating flow regime was evaluated and axial voidage profiles along the riser for different flow regimes were characterized as a function of gas velocities and mass fluxes. .

Introduction

Circulating fluid bed technology has been applied commercially to power generating, petroleum refining, and various chemical industries. This is a direct result of this technology to produce a plug flow, yet well mixed, and high throughput reactor. While there is extensive literature on circulating fluid bed (CFB) operating regimes (Yerushalmi and Cankurt, 1979; Teo, and Leung, 1986; Karri and Knowlton, 1991; Zijerveld et al., 1998; Bi and Fan, 1991; Bi and Grace, 1995), the ability to effectively scale these systems in size, geometry, and operating conditions are difficult because of the extensive deviation from ideal dilute gas-solids flow behavior. Hydrodynamic models are either too simple to incorporate the various operating regime transitions and reactor configuration limits, or so complex and time-consuming that adequate development and validation could only recently be undertaken due to their great demand for computational resources. Two fluid computations shows promise of accurate simulating hydrodynamics in the riser circulating fluid bed; however computational times are long due to the inherent large reactor systems and required grid-sizes comparable to the particle size (Guenther et al., 2002).

There is little available data in reactors large enough so that geometry (i.e. entrance, exit, and wall) effects do not dominate the hydrodynamics, yet with sufficiently large particle sizes to allow sufficiently large grid sizes to allow accurate hydrodynamic simulations. To meet this need experimental tests were undertaken with relatively large particles of narrow size

distribution in a large enough unit to reduce the contributions of wall effects and light enough to avoid geometry effects. While computational fluid dynamic are capable of generating detailed velocity and density profiles, it is believed that the validation and model development begins with the ability to simulate the global flow regime transitions. The purpose of this research is to generate well-defined test data for validation and begin to identify and measure critical parameters needed for these simulations.

Table 1. Riser dimensions and bed materials properties.

Cork characteristics:		
ρ_s	kg/m^3	189
ρ_b	kg/m^3	95
d_{p50}	μm	1170
d_{sv}	μm	812
U_t	m/s	0.86
U_{mf}	m/s	0.07
ε_{mf}		0.49
ϕ		0.84
Riser dimensions:		
H_{riser}	m	15.45
D_{riser}	m	0.305

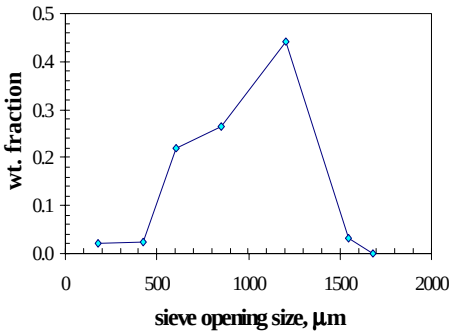

Figure 1. Typical size distribution of cork bed material.

Experimental Methods

A relatively light bed material was selected to generate data relevant for advanced high-pressure coal conversion processes. According to Buckingham-Pi analysis of the riser in a CFB the ratio of gas: solids density is critical factor important in scaling from a model, such as these cold flow tests, to a prototype application, such as a high pressure and high temperature transport reactor (Ghordzoe et al., 2001). Cork offers an excellent bed material which when tested at ambient conditions in air yields a similar density ratio to that of coal converted at 10-20 atmospheres and 1000 C. In addition, the shape factor for this natural wood material is expected to be comparable to that of coal that was derived from woody tissues and retains much of its morphology.

Riser dimensions and bed material properties are presented in Table 1. The particle density was measured using water displacement taking care to wet the surface completely. The cork surface is sufficiently hydrophobic to avoid filling any porosity with water. The particle size was measured using standard sieve analysis. The size distribution is displayed in Figure 1. The minimum fluidization velocity was measured in the loopseal by closing the slide gate valve in the standpipe and increasing the gas velocity while measuring an incremental presure drop. The sphericity was estimated fitting the Ergun equation to the pressure drop versus velocity profile taken prior to fluidization. The terminal velocity was calculated from drag laws using the measured solids density and particle size, and sphericity.

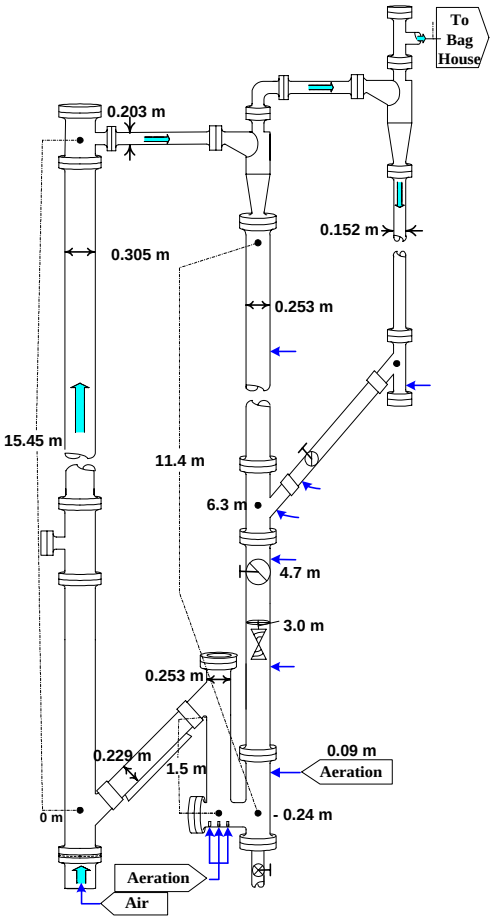

Figure 2. Schematic of CFB test unit indicating gas-solids separation and aeration location.

The test unit configuration is described by Monazam et al. (2001) and shown in Figure 2. The riser is constructed of flanged steel sections with one 1.22-m acrylic section install 2.44-m above the solids feed location. The solids enter the riser from a side port 0.23-m in diameter and 0.27-m above the gas distributor. Solids exit the riser through a 0.20-m port at 90^o about 1.2-m below the top of the riser at a point 15.45-m above the solids entry location (centerline to centerline). Riser velocities were corrected for temperature and pressure as measured at the base of the riser. The air's relative humidity was maintained between 40 and 60% to minimize effects of static charge building up on the solids. Zero offsets in pressure measurements were corrected by subtracting a baseline pressure profile across the riser with gas flow prior to circulating solids. Flows utilized did not produce any significant pressure drop due to gas flow. Twenty incremental differential pressures were measured across the length of the riser using transmitters calibrated within 0.1 % of full-scale or about 2 Pa/m. The primary response measurement was the overall riser pressure differential and it was calibrated within 0.45 Pa/m. Mass circulation rate was continuously recorded by measuring the rotational speed of a twisted spiral vane located in the packed region of the standpipe bed (Ludlow et al., 2002). This calibrated volumetric measurement was converted to a mass flux using the measured packed bed density presented in Table 1 and assuming that the packed bed void fraction at the point of measurement is constant (i.e. ε_b =0.45). Analysis of the standpipe pressure profile, estimated relative gas-solids velocities, and bed heights have indicated that this constant voidage estimate is reasonable over the range of operating conditions reported here.

Test data was collected over a period of 3 months. Operating conditions were varied by adjusting the riser flow or solids circulating rate while maintaining constant system outlet pressure at 0 psig. The solids circulation was varied by controlling the aeration at the base of the standpipe and by adjusting the total system inventory to increase the standpipe height. Steady state conditions were defined as holding a constant set of flow conditions and maintaining a constant response in the pressure differentials over a five-minute period. All steady state test results represent an average over that 5-minute period.

Results & Discussion

Reproducibility was characterized by comparing duplicate operating conditions. Differential pressure measurements are compared in Figure 3 for duplicate tests, Test No CK-14 and CK-16, with U_g of 4.9 m/s and G_s at 9.8 kg/m^2-s. The match of all of the measured points was extremely good. The primary error is associated with achieving identical operating conditions. These points were within 0.02 m/s and 0.03 kg/m^2-s. The pressure data were further analyzed by fitting an equation to the pressure profile along the riser length. This curve was numerically differentiated with respect to height and the differential pressures were assumed to be due to solids concentrations using the solids particle densities in order to convert the differential pressures to voidage (Monazam et al., 2001).

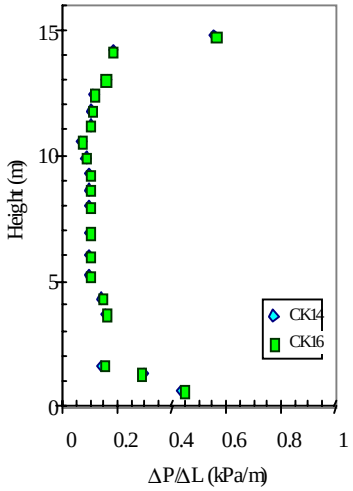

Figure 3. Riser incremental pressure profile for duplicate test

In order to identify the operating conditions several tests and data analyses were performed. The voidage profiles were characterized as a function of operating conditions. For a given gas velocity the solids circulation rate was increased. In the fast fluid bed regime the voidage profile changed from C-shape profile to S-shape up to homogenous or uniform axial profile (Figure 4A). The decrease in solids fraction at the bottom of the riser C-shaped profile was fit an exponential equation as developed by Kunii and Levenspiel (1990), while the S-shaped profile was fit to the equation presented by Li and Kwauk (1980). When operating with the riser in the S-shaped profile the voidage at the bottom of the riser does not change appreciably as long as the riser velocity is constant as reported by King (King, 1989). Once the S-shape profile is fully developed with a constant solids fraction at the bottom and top, gradually increasing the circulation rate results in an increased dense bed height. In other words the inflection point between the dense and dilute increases, up to a circulation rate characterized by a riser that is fully filled with dense bed.

At a higher gas velocity (Figure 4B) the range of mass fluxes that produced S-shaped profiles decreased. The transition from dilute to fully filled dense bed was narrower. The height of the acceleration zone at the bottom and length of the dense bed at the top depends upon the particle's terminal velocity and the gas velocity. At lower velocity the

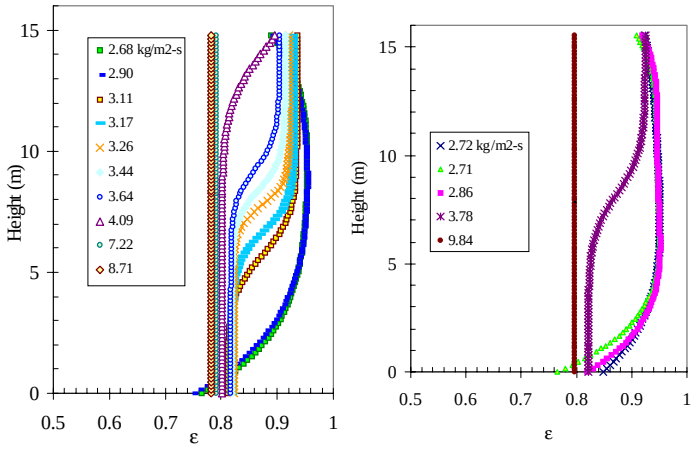

A) B)

Figure 4. Voidage profiles as a function of mass flux for two gas velocities: A) 3.2, and B) 3.4 m/s.

acceleration zone was pronounced - extending over 5 m up the length of the riser. As might be expected, this acceleration zone was shorter at the higher gas velocity. When sufficient mass flux is introduced to the riser the acceleration zone disappears or rather is converted to a uniformly dense bed region over a considerable length at the bottom of the riser.

At the low flow case the solids fraction near the exit nearly doubled compared to the solids fraction in the middle of the riser. This increased solid loading near the exit occurred only when operating below the fully developed S-shaped profile. But in the high flow case the solids fraction at the outlet was only about 25% greater than that in the middle of the riser. The exit effect was less prominent for the higher gas velocity. This trend tends to reverse itself when operating well above the terminal velocity of solids.

The transition from C-shaped riser solids profile to S-shaped can be measured by halting the solids flow, when the riser in a fully developed S-shaped profile (Monazam et al., 2001). The transient test data is then analyzed by taking the first derivative of the riser pressure drop with respect to time. The associated mass flux value at time=0 is referred to as the Saturation Carrying Capacity (SCC) because this is the most solids that a given velocity of gas can carry within the Fluid-Dominated (FD) regime (Li, 1994) without collapsing and forming a denser bed and entering the Particle-Fluid Compromising (PFC) regime (Li, 1994).

A comparison between the SCC and the steady-state mass flux revealed close agreement (Table 2); with the SCC was always slightly lower than the steady-state solids flux. This is because the SCC represents the upper limit for the FD regime and the lower boundary for the PFC regime. The dependence of the SCC with gas velocity is presented graphically in Figure 5. There was only a relatively small range of conditions that produced an S-shape riser pressure profile. Above 3.4 m/s the cork did not produce a discernible S-shaped riser profile. This may be a result of the corks narrow-size distribution or relatively large cork particles compared to PVC and coke materials studied previously. The transport velocity is thought to be above this point where no dense bed or S-shaped profile can be formed. However, an accurate determination of the transport velocity is difficult experimentally.

Table 2. Saturated Carrying Capacity (SCC) as measured from solids cut-off experiments at various Steady State (SS) test periods.

		riser at SS	SS	SCC
test no.	U_g(m/s)	$\Delta P/\Delta L$ (Pa/m)	G_s (kg/m^2-s)	G_s (kg/m^2-s)
ck48	2.81	217	2.50	1.96
ck71	2.94	226	2.44	2.20
ck138	3.09	232	3.45	3.07
ck128	3.24	232	3.78	3.61
ck129	3.39	207	4.82	4.65

The correlation developed by Monazam et al. (2001) was applied to this cork data and is also presented in Figure 5. The correlation was found to be quite sensitive to the cork terminal velocity. An error of only 5% in the displaced water volume during the measurement of the solids particle density produced sufficient variation in the sphericity to bring the correlation and SCC into excellent agreement due to the effect on the terminal velocity. Thus, it is apparent that simple calculation of the terminal velocity based on often-time difficult measurement of particle properties can lead to large inaccuracies.

As indicated above, the void fraction in the dense section at the base of the riser when operating in the S-shaped profile is function of gas velocity. Thus, the maximum pressure that can be generated in a riser of fixed height is also a function of U_g. Experimentally this maximum pressure drop can be calculated knowing the solids fraction in the dense bed of the riser in the S-shaped or dense regime using the following equation:

$$\Delta P_{r,max} = \rho_s \cdot (1-\varepsilon_{dense}) \cdot H_{riser}$$

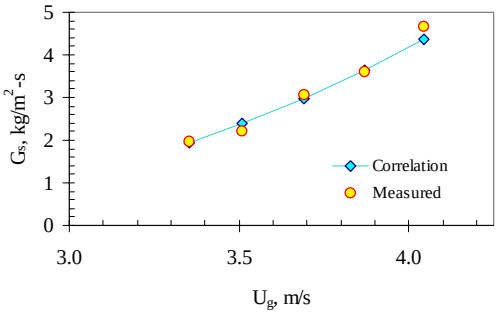

Figure 5. Saturated carrying capacity as measured for cork using solids cut-off tests compared to estimates from SCC correlation (Monazam, 2001).

a)

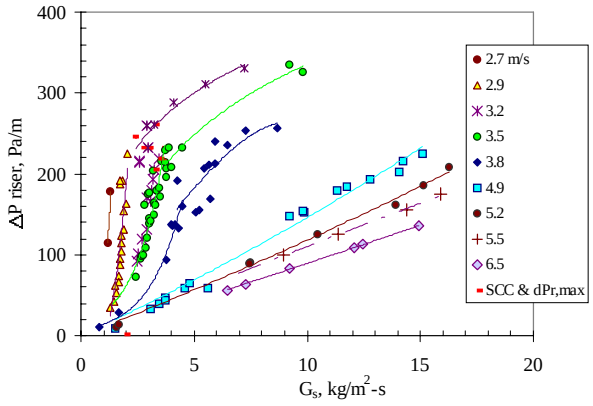

b)

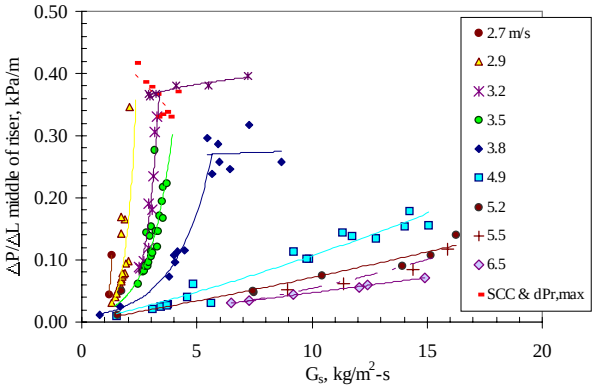

Figure 6. The variation in ΔP/ΔL with solids flux and gas velocity over A) the entire riser, and B) a 1.2 m increment at 2.44 m height at the base of the riser.

As expected the maximum riser ΔP/ΔL was always greater than that of the steady state and this value decreased slightly with increasing gas velocity. The transport velocity can be thought of as the point where the increasing SCC with increasing U_g intersects the line of decreasing maximum pressure drop in the riser with increasing U_g.

The operating regime can be mapped in several different coordinates. In Figure 6 the solids flux was varied over a series of constant riser gas velocities and the response variable was the solids inventory in the riser as measured by the riser ΔP/ΔL. When the ΔP/ΔL was analyzed over the base of the riser (6b) rather than across the entire riser (6a), a sharper transition between FD and PFC regimes was evident between 3.8 and 4.9 m/s. The $\Delta P_{r,max}$ clearly demarcated the transition between dilute flow with developing acceleration zone and a fully developed dense bed.

In Figure 7 the operating regime was mapped by plotting riser ΔP as a function of the gas velocity for a series of constant solid fluxes. In Figure 7a we display the range of solids fluxes lumped together. The line in Figure 7a represents the measured SCC. From Figure 7b it was

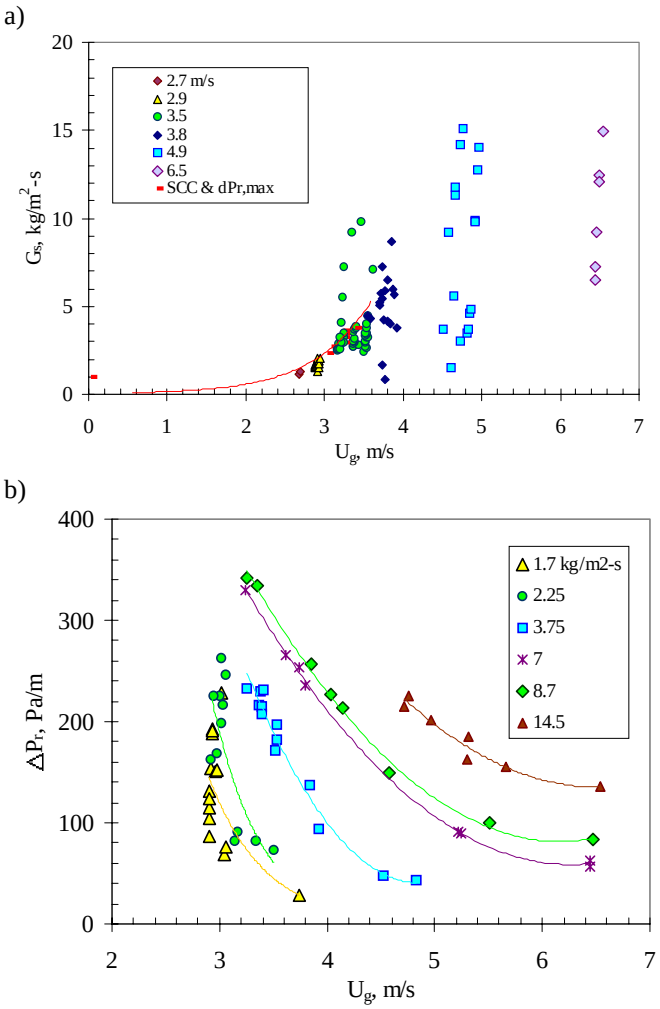

Figure 7. Variation of (a) Solids flux and (b) riser pressure on gas velocity for cork.

apparent that the cork tests were conducted in the solids dominated flow regime. In other words the riser pressure drops were dominated by solids inventory while the contribution from dynamic and static gas pressure was minimal. Only at the higher velocities did the pressure drop appear to approach the minimum in the classical Zenz $\Delta P - U_g$ plot signifying an approach to the gas friction dominated flow regime (Zenz and Othmer, 1960).

Summary

Identification of fluidization flow regimes and their boundaries is critical to CFB operation and performance. In this work the flow regimes were studied from homogeneous dilute-phase flow regime to dense-phase fluidization flow regime for a relatively coarse cork particle. This material was chosen to scale the density ratio for a coal gasifier. Interpretation of results in time domain pressure differentials and solids circulation data were used to identify the flow regimes by estimating the key operating regime transition, the SCC. Evaluation of particle terminal velocity was found to be critical to accurate SCC predictions. The operating regime was evaluated in several coordinates considering solids concentration profiles, and solids and gas fluxes. The axial solids profiles along the riser were characterized as a function of gas velocities and mass fluxes spanning three operating regimes.

Notation

$d_{p,50}$ mean particle size at 50 at percent (μm)
d_{sv} Sauter mean particle size (μm)
D riser diameter (m)
G_s solids flux (kg/m^2s)
H riser height (m)
P pressure (kPa)
SCC saturated carrying capacity (kg/m^2s)
U_g superficial gas velocity (m/s)
U_{mf} minimum fluidization velocity (m/s)
U_t particle terminal velocity (m/s)

Greek letters

ΔP_r pressure drop across the riser (kPa)
$\Delta P/\Delta L$ pressure drop per unit length (Pa/m)
ε voidage
ε_a limiting voidage of the dense phase
ε_{mf} voidage at minmum fluidization (m/s)
ρ_s solid particledensity (g/cc)
ρ_b bulk density (g/cc)
ϕ particle sphericity

Acknowledgments

The authors would like to acknowledge the Gasification Technologies, Combustion Systems, and Advanced Power Research Product lines of the U.S. Department of Energy for funding various aspects of this research.

References

Bi, H. T. & L. S. Fan, "Regime Transitions In Gas-Solid Circulating Fluidized Beds", AIChE Annual Meeting, Los Angeles, 17-22, November, (1991).

Bi, H. T. and J. R. Grace, "Flow Regime Diagrams for Gas-Solid Fluidization and Upward Transport", International Journal of Multiphase Flow, **21**, 1229(1995).

Ghordzoe, E, P. Smith, P. Vimalchand, G. Lui, and J. Longanbach, " Initial operations of the PSDF Transport Gasifier", Proceedings of the 16th International Conference on Fluidized Bed Combustion, FBC01-0065, Reno, Nevada, 2001.

Guenther, C., M. Syamlal, L.J. Shadle, C. Ludlow, **"**A Numerical Investigation of an Industrial Scale Gas-Solids CFB", submitted to the 7th International Circulating Fluid Bed Conference, Niagara Falls, Canada, 2002.

Karri, S. B. R. and T. M. Knowlton, " A Practical Definition of the Fast Fluidization Flow Regime", Proceedings of the Third International Conference on Circulating Fluidized Beds, ed. by P. Basu, M. Horior, and M. Hasatani, Pergamon Press, New York, 67-72(1991).

King, D.F., "Estimation of Dense Bed Voidage in Fast and Slow Fluidized Beds of FCC Catalysts", in *Fluidization VI*, ed. by J.R. Grace, L.W. Shemilt, and M.A. Bergougnou, New York, 1(1989)

Kunii, D.; and O. Levenspiel, Powder Technology, **61**,1990(1993).

Li, Jinghai, "Modeling" in *Advances in Chemical Engineering, Volume 20, Fast Fluidization*; ed. by M. Kwauk, , Academic Press, Inc., San Diego, 148(1994).

Li, Y.C.; and M. Kwauk, "The Dynamics Of Fast Fluidization"; in *Fluidization*, ed. by J.R. Grace, and J. M. Matsen , Plenum Press, New York, 537(1980).

Ludlow, C., L. O. Lawson and L. J. Shadle, "Development of a Spiral Device for Measuring the Solids Flow in a Standpipe", submitted to the 7th International Circulating Fluid Bed Conference, Niagara Falls, Canada, 2002.

Monazam, R.E.; L.J. Shadle; and L.O. Lawson, "A Transient Method for Determination of Saturation Carrying Capacity", accepted for publication in Powder Technology, 2001.

Teo, C. S. and L. S. Leung, "Vertical Flow of Particulate Solids in Standpipes and Risers", in *Encyclopedia of Fluid Dynamics, Volume 4. Solids and Gas-Solids Flows*, ed. by N. P. Cheremisioff, Gulf Publishing Company, Houston, 611(1986).

Yerushalmi, J.; and N.T. Cankurt, "Further Studies of the Regimes of Fludization", Powder Technology, **24,** 187(1979).

Zenz, F. A. and D. F. Othmer, *Fluidization and Fluid Particle Systems*, Reinhold Publishing Corp., New York, 318(1960).

Zijerveld, R. C., F. Johnson, A. Marzocchella, and J. C. Schouten, "Fluidization Regimes and Transitions from Fixed Bed to Dilute Transport Flow", Powder Technology, **95**, 185(1998).